◆ Human Brain Mapping 31:1675–1685 (2010) ◆

Electrophysiology Meets fMRI: Neural Correlates of the Startle Reflex Assessed by Simultaneous EMG–fMRI Data Acquisition

Irene Neuner,[1,2,3]* Tony Stöcker,[2,3] Thilo Kellermann,[1,3] Veronika Ermer,[2,3] Hans Peter Wegener,[4] Simon B. Eickhoff,[1,3,5] Frank Schneider,[1,3,6] and N. Jon Shah[2,3,6,7]

[1]*Department of Psychiatry and Psychotherapy, RWTH Aachen University, 52074 Aachen, Germany*
[2]*Institute of Neuroscience and Medicine-4, Forschungszentrum Juelich GmbH, 52425 Juelich, Germany*
[3]*JARA—Translational Brain Medicine, Juelich, Germany*
[4]*Central Institute of Electronics, Forschungszentrum Juelich GmbH, 52425 Juelich, Germany*
[5]*Institute of Neuroscience and Medicine-2, Forschungszentrum Juelich GmbH, 52425 Juelich, Germany*
[6]*Brain Imaging Centre West, 52425 Juelich, Germany*
[7]*Department of Neurology, RWTH Aachen University, 52074 Aachen, Germany*

Abstract: The startle reflex provides a unique tool for the investigation of sensorimotor gating and information processing. Simultaneous EMG–fMRI acquisition (i.e., online stimulation and recording in the MR environment) allows for the quantitative assessment of the neuronal correlates of the startle reflex and its modulations on a single trial level. This serves as the backbone for a startle response informed fMRI analysis, which is fed by data acquired in the same brain at the same time. We here present the first MR study using a single trial approach with simultaneous acquired EMG and fMRI data on the human startle response in 15 healthy young men. It investigates the neural correlates for isolated air puff startle pulses (PA), prepulse–pulse inhibition (PPI), and prepulse facilitation (PPF). We identified a common core network engaged by all three conditions (PA, PPI, and PPF), consisting of bilateral primary and secondary somatosensory cortices, right insula, right thalamus, right temporal pole, middle cingulate cortex, and cerebellum. The cerebellar vermis exhibits distinct activation patterns between the startle modifications. It is differentially activated with the highest amplitude for PPF, a lower activation for PA, and lowest for PPI. The orbital frontal cortex exhibits a differential activation pattern, not for the type of startle response but for the amplitude modification. For pulse alone it is close to zero; for PPI it is activated. This is in contrast to PPF where it shows deactivation. In addition, the thalamus, the cerebellum, and the anterior cingulate cortex add to the modulation of the startle reflex. *Hum Brain Mapp 31:1675–1685, 2010.* © 2010 Wiley-Liss, Inc.

Additional Supporting Information may be found in the online version of this article.

Contract grant sponsor: Bundesministerium für Bildung und Forschung (BMBF); Contract grant numbers: BMBF 01GO0104 (to N.J.S. and Karl Zilles), BMBF 01GO0204 (to Brain Imaging Centre West); Contract grant sponsors: Medical Faculty of the RWTH Aachen University ("Rotationsprogramm"; to I.N.).

*Correspondence to: Irene Neuner, M.D., Department of Psychiatry and Psychotherapy, RWTH Aachen University, Pauwelsstr. 30, 52074 Aachen, Germany. E-mail: ineuner@ukaachen.de

Received for publication 27 March 2009; Revised 7 August 2009; Accepted 12 November 2009

DOI: 10.1002/hbm.20965
Published online 4 March 2010 in Wiley Online Library (wileyonlinelibrary.com).

Key words: neurophysiology; fMRI; startle reflex; MR artifact correction; prepulse inhibition; prepulse facilitation

INTRODUCTION

The startle reflex and its modification via prepulses provide an important window on the basic principles of information processing [Graham, 1975; Koch and Schnitzler, 1997; Swerdlow et al., 2001a]. If the startle pulse is preceded by a weaker, nonstartling pulse in a time range of 40–400 ms, the startle eye blink will be inhibited, which is termed prepulse inhibition (PPI) [Blumenthal, 1996; Braff et al., 1992; Swerdlow et al., 1999, 2001a]. If the time range between the prepulse and the startling pulse is either very small (<20–40 ms) or large (>1,000 ms), the startle response is facilitated [prepulse facilitation (PPF); Graham, 1975; Hsieh et al., 2006]. PPI and PPF are thought to reflect two different mechanisms. The amount of PPI is interpreted as an index of automatic sensorimotor gating and hence indicative of a protection mechanism in sensory processing [Graham, 1975; Swerdlow et al., 2001a; Swerdlow and Geyer, 1998]. The mechanism underlying PPF is less clear. Graham [1975] discussed that facilitation produced by a sustained prepulse is at least in part the result of generalized arousal processes elicited by the prepulse. Although the elicitation of the startle blink is an automatic process which does not require attentional processing, it can be reliably modified by attentional processing of the prepulse [Filion et al., 1993]. As reviewed by Braff et al. [2001], theories about the neural correlates of the startle reflex and its modification historically first embraced the concept that sensory information is processed through a series of sequential "steps" or "stages." Later, these "stage" models were increasingly challenged by evolving "integrationist" models of neural networks, which emphasize that parallel information processing in multiple loci is integrated into a "symphonic array" of time-coordinated events [Braff et al., 1999, 2001].

The primary startle circuit as described by Davis et al. [1982] in rats consists of six synapses: the auditory nerve, the posterioventral cochlear nucleus, the ventral nucleus of the lateral lemniscus, the nucleus reticularis pontis caudalis, spinal interneuron, and finally the lower motor neuron. PPI of the startle response in rats is regulated by a number of neural structures including the hippocampus, the prefrontal cortex including the medial prefrontal cortex and orbital cortex, the basolateral amygdala, the core and shell of the nucleus accumbens, the basal ganglia, the thalamus (mediodorsal nucleus, medial geniculate), the ventral tegmental area, the substantia nigra reticulate, and the peduncolopontine nucleus [Braff et al., 2001]. This limbic cortico-striato-pallido-pontine circuitry converges with the primary startle circuit at the level of the nucleus reticularis pontis caudalis [Braff et al., 2001]. Unlike PPI, the anatomical substrates of PPF are poorly described [Plappert et al., 2004]. Research on PPF seems to be limited to pure electrophysiological studies including the investigation of influences of background noise and interstimulus interval pulse–prepulse [Davis et al., 1982; Fendt, 2001; Koch and Schnitzler, 1997; Plappert et al., 2004; Takahashi et al., 2007].

In comparison to electrophysiological studies, only few neuroimaging studies using fMRI and PET to investigate the startle reflex and its modification have been carried out so far [Campbell et al., 2007; Goldman et al., 2006; Hazlett et al., 1998, 2001, 2008; Kumari et al., 2003a,b]. Most studies focus on the neural correlates of PPI reporting a complex neural network made up of a primary pontine circuitry that interconnects with inferior parietal, superior temporal, and prefrontal cortices via thalamus and striatum. Campbell et al. [2007] report bilateral PPI-related BOLD responses in the caudate nuclei, the left insula, the right middle frontal gyrus, and right fusiform gyrus. When the mean startle amplitude for PPI was included in the fMRI analysis as a covariate, activation clusters were identified in the caudate nuclei, the thalamic nuclei, the anterior cingulate cortex, the pons, and the left angular gyrus [Campbell et al., 2007]. Kumari et al. [2007] report increased activity in the striatum, thalamus, insula, hippocampus, temporal, inferior frontal, and inferior parietal regions associated with PPI. These studies contribute important insights into the neural correlates of the startle reflex and its modification for PPI via a fronto-striatal thalamic circuitry [Hazlett et al., 2008]. To our knowledge, there is no published neuroimaging study investigating PPF. FMRI startle studies reported by Kumari et al. [2003a,b] or Campbell et al. [2007] stimulate simultaneously but do not record simultaneously. The influence of different parameters such as background noise level and habituation from one session to the other as opposed to data gathered within one session is significant [Blumenthal, 1996; Hsieh et al., 2006; McDowell et al., 2006]. Until now, real simultaneous approaches, i.e. simultaneously stimulate and record startle responses, have been limited to the PET environment [Hazlett et al., 1998].

Simultaneous stimulation and recording allows one a quantitative assessment of the startle response and the corresponding BOLD response in analogy to EEG/fMRI-data analysis on a single trial level [Esposito et al., 2009, in press; Mulert et al., 2008]. The single trial results of the individual startle measurement enter the statistical analysis of the event-related fMRI data and add valuable information which is otherwise lost. This enables the identification of neural components implicated in the regulation of the startle reflex and its modification. FMRI-

startle paradigms using pharmacologic challenges would especially profit from simultaneously acquired data. The simultaneous measurement would help quantify the extent of deficient inhibition via PPI measurement and assess the effect of pharmacological intervention. A broad range of neuropsychiatric disorders such as schizophrenia, Tourette's syndrome, and Huntington's disease is characterized by a deficit in gating out irrelevant stimuli or a lack of inhibition.

The online, simultaneous measurement of the startle reflex mandates MR-compatible EMG electrodes, electrode leads, and amplifiers. In addition, the switching of the MR gradient coils causes severe interference patterns in the recorded EMG signal. The startle set up in the MR scanner is further complicated by the issue of stimulation. The balance between acoustic stimulation being loud enough to elicit the startle reflex but still safe for the volunteer during fMRI is a difficult one to attain. We therefore adapted air puff stimulation for use in the MR scanner. The use of air puff stimulation has been reported by Swerdlow and colleagues [Kumari et al., 2003c; Swerdlow et al., 2001b] as a successful MRI-friendly approach.

In this study, an MR-compatible EMG startle set up is described which meets the above challenges. With this combined study approach we aimed to answer the following questions:

a. Which neural structures form the core neural network for processing PA, PPI, and PPF? More precisely, the pulse alone (PA) is regarded as "default" or control condition, whereas it is assumed that both prepulses (PPI and PPF) engage brain areas more than the PA does. Based on the results of animal research [Braff et al., 2001] and available neuroimaging studies we hypothesize a pontine network connecting via thalamus and striatum to prefrontal, parietal, and temporal cortical areas [Goldman et al., 2006; Hazlett et al., 1998, 2001; Kumari et al., 2003a,b,c, 2007]. This network will receive additional contributions from the cerebellum, the hippocampus, amygdala, insula, and cingulate cortex [Braff et al., 2001; Campbell et al., 2007; Goldman et al., 2006; Hazlett et al., 1998, 2001, 2008; Kumari et al., 2003a,b,c; Timmann et al., 1998].
b. Which neural structures are differentially involved in the PA, PPI, and PPF? This is a rather explorative approach, since—as far as we know—no imaging study has yet compared the startle reflex and both modification types in one experiment. To our knowledge PPF has not even been investigated with neuroimaging techniques yet.
c. Which neural structures show activity that is related to the amplitude of the startle response? Candidate structures for the modulation of startle amplitudes based on prior studies and animal research are the prefrontal cortex, the nucleus caudate, the anterior cingulate cortex, and the thalamus [Campbell et al., 2007; Hazlett et al., 2001; Kumari et al., 2003a,b,c; Swerdlow et al., 2001a].

MATERIALS AND METHODS

Healthy Subjects

We included 15 male subjects (aged 21–41 years, mean 28.4, SD 6.2) for the analysis of electrophysiological and fMRI data (out of 22 scanned subjects five were excluded due to startle nonresponsiveness and two subjects due to realignment parameters exceeding the limit of 2 mm). Nonresponsiveness was defined as two or more responses missing in Section A or unusable PPI or PPF data, e.g., the responses were too low to be clearly distinctive from baseline. A board-certified neurologist and psychiatrist screened subjects by clinical interview. Exclusion criteria were intake of any medication, recreational drug use, or any past or present history of neurological or psychiatric disorders, as well as relatives of first degree suffering from psychiatric disorders. All subjects gave written informed consent. The study was approved by the local ethics committee. Subjects received a monetary compensation (15 € per hour) for their participation.

Startle Recording Set-Up

The set-up for recording the subjects' startle reflex inside the scanner consisted of an MR-compatible EEG amplifier (MR plus, Brainproducts, Munich, Germany) and a custom-made, adjustable MR-compatible EEG cap (Easy cap, Munich, Germany). The startle reflex was recorded from the right orbicularis oculi muscle. Electrodes for recording electromyographic activity of this muscle were fixed below the eye in midline and the outer canthus. The ground electrode was positioned at Iz. Prior to placement of the electrodes, the skin was treated with alcohol and abralyte^{TM} gel (EasyCap, Munich, Germany) to reduce resistance below 10 kΩ.

Air Puff Stimulation

Given the limitation of using auditory stimulation for evoking startle responses, we chose to use somatosensory stimulation by means of air puffs to elicit the startle reflex. Two custom-made flexible plastic mountings were attached to the left rail of the scanner table, each containing a Teflon tube of 6 mm diameter (see Fig. 1). These were individually bent for each subject to point to the region below the left clavicula. The Teflon tubes were fed through a wave guide from the scanner room to the neighboring technical room and each one was connected to a pressure regulator. The first pressure regulator was set to 8 PSI and the second one to 40 PSI. The magnetic valves of the pressure regulators were triggered

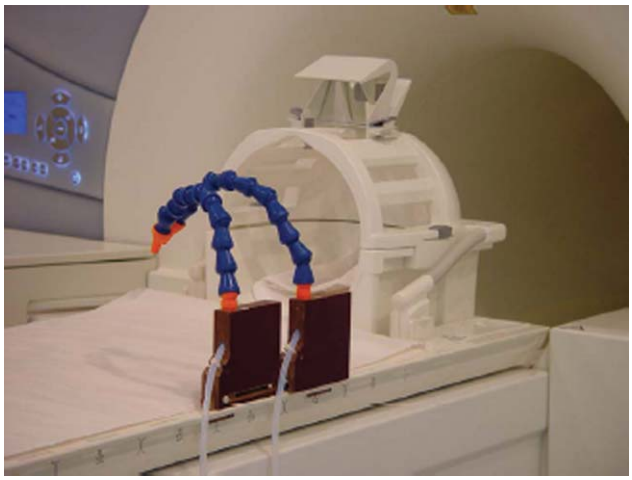

Figure 1.
Set up of the air puff stimulation in the MR suite. Blue plastic mountings are flexible and allow for individual adaptation. [Color figure can be viewed in the online issue, which is available at wileyonlinelibrary.com.]

by a control element connected to the PC governing the timing of the stimuli via the presentation software package.

Stimulation Paradigm

To be consistent with the conventional setup for testing the startle reflex, the experimental stimulation was preceded by a rest period in the scanner. This lasted for 5 min and allowed for adaptation to the scanner surroundings and noise of the running EPI sequence. During this 5-min-period no air puff stimulation was delivered. The subjects lying in the scanner were instructed to keep their eyes open throughout the experiment and to focus on a blue stripe at the upper border of the magnet bore and tolerate the air puffs passively. The air puff stimuli were presented in an event-related design in three different successive sections, A, B, and C. In Section A, six PA stimuli (40 PSI, duration 20 ms) were delivered at an interstimulus interval jittered between 9.3750 and 28 s. In Section B, 18 PA stimuli, 18 PPI stimuli (prepulse: 8 PSI, duration 20 ms, pulse as in PA, prepulse–pulse interval 140 ms) and 18 PPF stimuli (prepulse: 8 PSI, duration 20 ms, pulse: 40 PSI, duration 20 ms, prepulse–pulse interval 4,500 ms) were delivered in a random order at an interstimulus interval jittered between 9.3750 and 28 s. The order and onsets of the stimuli in this section were calculated using the program optseq (http://surfer.nmr.mgh.harvard.edu/optseq/). In Section C, six PA stimuli were applied again. In total, the event-related experiment consisted of one session starting with a rest period followed immediately by Sections A, B, and C for a total scan duration of 24 min.

MR Protocol

The study was performed using a 3T Tim Trio Scanner (Siemens, Erlangen, Germany) at the Research Center Juelich. Prior to the startle experiment, an anatomical MR scan was obtained using the MP-RAGE sequence at an isotropic resolution of 1 mm. For functional MRI, an EPI sequence with a 64 × 64 imaging matrix, FOV of 200 mm, TR of 2,500 ms, TE of 30 ms, and 40 slices with slice-thickness 3 mm and 10% slice gap was applied. Five hundred seventy-six EPI volumes were acquired within the complete run.

Startle Data Analysis

Offline data analysis was performed with Brainvision Analyser Version 1.3 (Brain Products, Munich, Germany). Raw data underwent corrections for MR-gradient artifacts and cardioballistic artifacts [Allen et al., 1998, 2000]. Independent component analysis was applied to extract startle responses. For each startle response, the onset latency, peak-to-peak amplitude, and peak latency were calculated. For latency measurements, the first peak after onset was chosen. For startle reactivity, we averaged all PA trials of Section A. Nonresponsiveness was determined when at least two PA trials did not elicit a startle response in Section A. Assessment of startle habituation was calculated by the average of the six PA trials in Section C divided by the average of the six PA trials in Section A. %PPI was calculated (PPI − PA)/PA * 100. %PPF was calculated (PPF − PA)/PA * 100.

fMRI Data Analysis

Prior to the fMRI data processing, data quality was assessed by means of the quality assurance protocol described by Stöcker et al. [2005], which provides the time series of global percent signal change (PSC) as a data quality measure. fMRI data proved to be of high quality with a mean PSC of 3.1% (SD 0.27). Thereafter, the data were analyzed using Statistical Parametric Mapping (SPM5, Wellcome Department of Cognitive Neurology, Institute of Neurology, University College of London, UK). The first 120 images, acquired during the rest period for scanner-noise adaptation, were discarded for this analysis. The remaining 456 images were corrected for between-scan movement by rigid-body realignment to the first image. After spatial normalization to the EPI template provided by the SPM package, the time series was spatially smoothed with an isotropic Gaussian kernel of 10-mm FWHM (full-width at half-maximum).

For the individual first-level analyses, the input functions representing the timing of each event type (PA, PPI, and PPF) in that subject were convolved with the canonical hemodynamic response function (HRF) to construct the regressors for a voxel-by-voxel analysis within the framework of the general linear model (GLM).

TABLE I. Results of startle measurements

Startle response	Magnitude	Peak–latency (ms)
PA mean sections A–C	2,274 μV (2,860 μV)	125 (24)
PA section A	5,243 μV (5,883 μV)	132 (24)
PA section B	1,695 μV (2,416 μV)	123 (20)
PA section C	1,601 μV (2,737 μV)	132 (57)
PPI	−37%	244 (42)
PPF	+55%	248 (28)

Additionally, regressors of temporal derivatives of each event-vector were included in the statistical model to account for temporal shifts in the individual BOLD response relative to its canonical form [Friston et al., 1998; Henson et al., 2002]. Furthermore, each of the three event-regressors, PA, PPI, and PPF, was parametrically modulated with the individual startle amplitudes. These parametric modulation (PM) vectors enter the SPM design matrix as additional columns. Thus, the statistical model allows for separation of general, condition-specific neuronal activations like PA, PPI, and PPF and of those effects that are correlated with the measured amplitude of the startle reflex, PAm (PA-modulated), PPIm (PPI-modulated), and PPFm (PPF-modulated) [Durston et al., 2003; Friston et al., 1998; Maguire et al., 2001]. Finally, the SPM realignment parameters and the data quality parameter PSC were introduced as additional covariates to remove movement-related variance from the time-series.

Frequencies below a period of 128 s were eliminated by means of a high pass filter to remove scanner drifts and the aliasing of physiological noise. Autocorrelations of the time-series were modeled using an autoregressive model as implemented in SPM5. Parameter estimates of the HRF for each event type (PA, PPI, and PPF) as well as their PMs with the startle response (PAm, PPIm, PPFm) from each subject were entered into a within-subject ANOVA. Model specification of the ANOVA allowed for dependencies between conditions and unequal variances between subjects and conditions. We calculated the following contrasts:

1. Planned t-contrasts (thresholded at $P < 0.05$, FWE corrected and using an extent threshold of 10 voxels) for PPI versus PA, PPF versus PA, PPIm versus PAm, and PPFm versus PAm. These contrasts aimed at identifying brain regions that are more engaged during each of the experimental conditions (PPA and PPI) as compared to the control condition (PA) (and the PMs, respectively). The underlying hypothesis is that the brain processes both prepulses (PPI and PPF) in a way that some regions are more active as they are when a PA is presented.
2. Conjunction analysis (thresholded at $P < 0.001$ uncorrected, whole brain and ROI approach based on probability maps [Eickhoff et al., 2005, small volume correction, $P < 0.001$] for PA, PPI, and PPF and in analogy for PAm, PPIm, and PPFm (thresholded at $P < 0.001$ uncorrected)
3. F-contrast "Differences PA, PPI, PPF" (thresholded at $P < 0.001$ uncorrected, extent threshold 50 voxel) spanning all differences between the condition regressors, i.e. testing simultaneously for any change in the neural activity between PA, PPI, and PPF, and F-contrast "Differences PM" (thresholded at $P < 0.001$ uncorrected, extent threshold 50 voxel), i.e. testing simultaneously for any change in the neural activity between PAm, PPIm and PPFm. In addition, we performed with a priori hypotheses for the candidate regions a region of interest (ROI) approach. ROIs were placed based on the results of the t-contrasts PPI versus PA, PPF versus PA, or the conjunction analysis (ROI sphere 20 mm, SVC $P < 0.05$ corrected at MNI −32 −52 −36, MNI 6 8 24, MNI 8 14 8, and MNI −8 14 8).

RESULTS

Startle Data

The relative PPI response were calculated by 100 × (PPI − PA)/PA, resulting in a mean percentage change of −37% for all inhibition events. Accordingly, the relative PPF response was calculated by 100 × (PPF − PA)/PA, resulting in a mean percentage change of +55% for all facilitation events. Habituation was calculated by dividing the mean PA amplitude in Section C through the mean PA amplitude in Section A. This showed a habituation effect of 70% (Table I).

fMRI Data Analysis

PPI versus PA

The contrast PPI versus PA shows activation in the right superior parietal lobe (MNI 44 −54 60) and the right inferior frontal gyrus, pars triangularis (MNI 44 −54 60).

PPF versus PA

The contrast PPF versus PA shows activation in the left superior medial gyrus (MNI −2 44 46), right middle frontal gyrus (MNI 32 24 56), anterior/middle cingulate cortex (MNI 6 8 24, 13 4 42) and the cerebellum [crus 1 left MNI −12 −70 −34, left cerebellum lobule IX MNI −8 −48 −50, right cerebellum (lobule VIII) MNI 24 −44 48].

PPIm versus PAm

The contrast PPIm versus PAm shows the right caudate nucleus (MNI −6 10 12), the right anterior cingulate cortex (MNI 16 22 24), the left superior medial gyrus (MNI −8 66

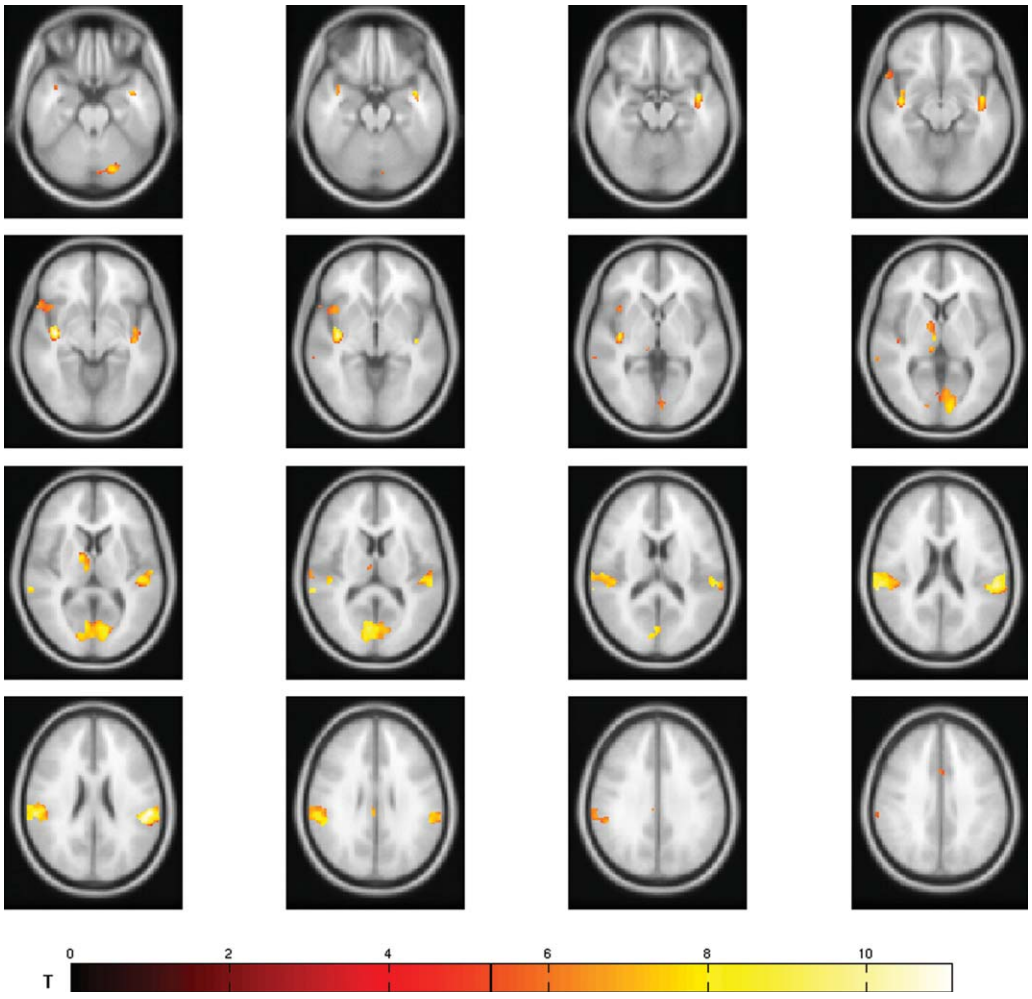

Figure 2.

The conjunction analysis PA–PPI–PPF reveals a common core network consisting of primary and secondary somatosensory cortices, the left thalamus, the right insula, the right temporal pole, the middle cingulate cortex, and cerebellar components.

14), and the right cerebellum (lobule VIII) (MNI −20 −62 −46).

PPFm versus PAm

The contrast PPFm versus PAm ($P < 0.001$, uncorrected, extent threshold 10 voxel) reveals cerebellar activation spots in the right lobule VIII and the left lobule X (MNI −14 −42 40, $t = 4.51$; MNI 20 −62 −46, $t = 3.8$).

Conjunction analysis PA–PPI–PPF

The conjunction analysis identified primary and secondary somatosensory cortices, the right thalamus, the right insula, the right temporal pole, the cerebellum, and the middle part of the cingulum as the essential common neural network for the startle reflex and its modification (see Fig. 2). Coordinates in MNI space are listed in Table II.

Conjunction analysis PAm–PPIm–PPFm

The conjunction analysis over PAm, PPIm, and PPFm revealed no suprathreshold voxels.

F-test differences PA-PPI-PPF

The F-contrast spanning all differences between the condition regressors, i.e. testing simultaneously for any change in the neural activity between PA, PPI, and PPF, reveals cerebellar activation in the vermis (MNI 4 −58 −32, $F = 7.23$, Fig. 3a). The contrast estimates are depicted in Figure 3b.

TABLE II. Conjunction analysis PA, PPI, and PPF

Macroanatomic region	MNI coordinates	*t* value	Probability[b]	Area[b]
Supramarginal gyrus R	58 −28 22	7.77	Probability 40%	OP1
	66 −24 22	7.48	Probability 40%	OP1
Superior temporal gyrus R	48 −28 16	6.78	Probability 70%	OP1
Superior temporal gyrus L	−50 −26 8	7.37	Probability 30%	TE1.0
			Probability 20%	TE1.1
Heschl's gyrus R	44 −20 6	5.55	Probability 60%	TE1.0
			Probability 30%	TE1.1
Insula lobe R	40 −14 −6	9.34		
	40 0 −10	5.51		
	44 14 −6	6.24		
Calcarine gyrus L	−12 −80 6	7.55	Probability 100%	Area 17
	−2 −82 10	6.46	Probability 80%	Area 18
Calcarine gyrus R	4 −74 10	6.7	Probability 70%	Area 18
	12 −84 10	6.40	Probability 100%	Area 17
Thalamus R	8 −14 8	6.26	P0.92 prefrontal cortex[a]	
	12 −2 6	7.12	P0.85 prefrontal cortex	
	10 −26 2	6.07	P0.36 prefrontal cortex	
			P0.45 post. parietal cortex	
	12 −28 4	6.03	P0.21 post. parietal cortex	
			P0.45 temporal cortex	
Cerebellum Crus 1 L	−16 −76 −26	6.84		
	−6 −80 −24	5.84		
Cerebellum lobule VI L	−32 −52 −36	5.84		
Middle cingulated cortex L	2 14 40	6.11		
Postcentral gyrus	6 −46 64	0.001 SVC	Probability 40%	Area3a
Amygdala	34 −5 −18	0.001 SVC	Probability 50%	Laterobasal amygdala
	−30 −3 −22	0.001 SVC	Probability 90%	Laterobasal amygdala
Hippocampus	18 −30 −7	0.001 SVC	Probability 70%	Subiculum
	−18 −31 −7	0.001 SVC	Probability 80%	Subiculum
Brainstem	1 −25 −21	0.001 SVC		

[a] Probability as assessed by Thalamic Connectivity Atlas, (http://www.fmrib.ox.ac.uk/cgi-bin/thalamus.pl, Behrens et al. 2003).
[b] Anatomy toolbox for SPM [Amunts et al., 2000, 2005; Eickhoff et al., 2005, 2006; Geyer et al., 1999; Morosan et al., 2001].

F-test differences PM

The F-contrast spanning all differences between the condition regressors, i.e. testing simultaneously for any change in neural activity between PAm, PPIm, and PPFm, reveals a frontal center of activation in the left middle orbital gyrus (MNI 0 58 −4, $F = 7.72$) (see Fig. 4a). Contrast estimates are shown in Figure 4b. The ROI approach showed significant small clusters in the left cerebellum (10 voxels, local maximum at MNI −16 −42 −40), in the anterior cingulum (Cluster 1: 28 voxels, local maximum at MNI −6 8 12; Cluster 2: 21 voxels, local maximum at MNI 16 22 34), and in the left thalamus partly overlapping in the striatum (Cluster 1: 4 voxels, local maximum at MNI −24 −20 0; Cluster 2: 13 voxels, local maximum at MNI −20 −6 4). Parameter estimates are provided in Supplementary Table 1.

DISCUSSION

Our simultaneous measurement (i.e., stimulation and recording) of fMRI and startle reflex identified primary and secondary somatosensory cortices, the right thalamus, the right insula, the right temporal pole, the cerebellum, and the middle part of the cingulum as essential common neural network for the startle reflex and its modification.

Despite air puff (i.e., somatosensory stimulation), primary acoustic and visual cortices show activation in the conjunction analysis for PA, PPI, and PPF. The acoustic activation could either result from the distinct hissing tone caused by the air puffs leaving the Teflon tubes or from the primary visual activation via crossmodal activation through the somatosensory stimulus [Diederich and Koch, 2005; Lugo et al., 2008; McDowell et al., 2006; Senkowski et al., 2008; Diederich and Colonius, 2008].

In our results PPI differs from PA in the additional recruitment of prefrontal and parietal areas. The recruitment of prefrontal areas for PPI is well in line with the results of animal research and prior neuroimaging findings. In their comprehensive review, Swerdlow et al. [2001a] describe the role of the prefrontal cortex including the medial prefrontal cortex and the orbital cortex. An ^{18}FDG-PET acoustic startle study in humans [Hazlett et al., 1998] supports the findings from research in rodents and

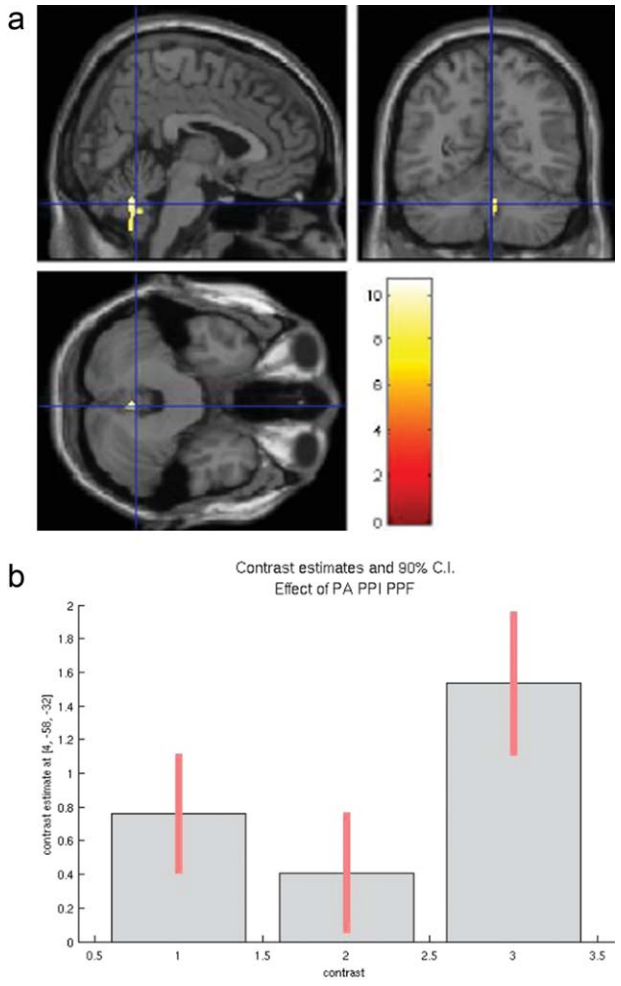

Figure 3.

(**a**) The F-contrast differences PA–PPI–PPF reveals cerebellar activation with maximum activity localized in the vermis. (**b**) The contrast estimates plot reflects high activation for PPF in comparison to PPI.

reports an association between a high PPI response and a high prefrontal glucose metabolism (Brodman areas 8, 9, und 10 bilaterally). Another group [Kumari et al., 2005] revealed a positive correlation between acoustic PPI and gray matter volume in the dorsolateral prefrontal, middle frontal, and orbital/medial prefrontal cortices. Our data indicate that for the modulation of PPI the left superior medial frontal cortex, the anterior cingulate cortex, the right caudate nucleus, and the cerebellum are of importance. A modulating role for the nucleus caudatus in PPI is also known from work in rats [Swerdlow et al., 2001a]. In humans, Campbell et al. [2007] report in their fMRI study at 1.5 T in combination with off-line recorded acoustic PPI an association between the startle amplitudes and the BOLD signal bilaterally in the caudate nuclei, the anterior cingulate cortex, the pons, the angular gyrus, and the thalamus. Our data replicate these data in a tactile paradigm for the caudate nucleus, the striatum, the thalamus, and the anterior cingulate. In contrast to Campbell et al., we did not replicate the association between pons activation and PPI response. In our data, in the brainstem, no activation cluster emerges for the differential t-contrast PPIm versus PAm. Only in the conjunction analysis using an ROI approach a small cluster is detected. However, this has to be interpreted with care. The imaging of the brainstem in fMRI is a demanding task, since during the cardiac cycle the brainstem moves in rostral–caudal direction 1–2 mm. Another challenge lies in the differentiation between reliable activation and signal artifacts originating from small veins. In future studies, these challenges can be met partly by the cardiac gating of the EPI sequence and

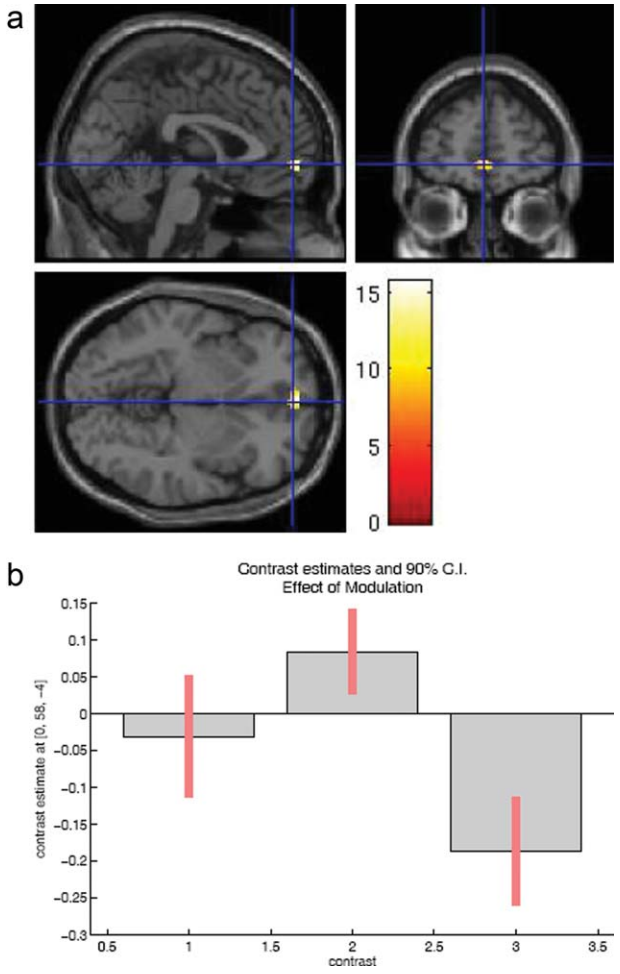

Figure 4.

(**a**) The F-contrast differences PM identifies frontal activation in the middle orbital gyrus. (**b**) For the startle modification it shows differential activation patterns, activation during PPI as opposed to deactivation during PPF.

increased sample size. In addition, we would adapt our image acquisition scheme in a way to use an interstimulus interval of 120 ms for PPI. In further studies, this would allow a better comparison to other studies in the literature. The interstimulus interval of 120 ms is important with regard to attentional influences on the startle reflex and its modification in active paradigms (e.g., with attention to prepulses) [Filion et al., 1993].

In their review, Swerdlow et al. [2001a] describe the involvement of the basolateral amygdala and the hippocampus in the regulation of PPI. A ROI approach confirms the participation of the basolateral amygdala and the hippocampus for the data of the conjunction analysis PA, PPI, and PPF. The implication of the amygdala in the regulation circuit of the startle response correlates well with psychophysiological measurements which show a potentiation of the startle response during aversive picture viewing as an indicator of trait fear [Vaidyanathan et al., 2009].

In contrast to PPI data PPF data in animals and humans are sparse. The actual underlying neural pathway is not well studied [Plappert et al., 2004]. In our human data, we find that PA, PPI, and PPF share a common core network. PPF differs from PA in our data by the recruitment of prefrontal areas, the anterior/middle cingulate cortex, and cerebellar activations.

Based on the differential activation pattern in the F-contrast for the modulated PA, PPI, and PPF measure, the orbital cortex seems to play an important role in the modulation of the startle responses (Fig. 3a,b). Our findings are supported by animal research and a lesion study in patients. Zavitsanou et al. [1999] report that dopamine antagonists in the orbital prefrontal cortex reduce PPI of the acoustic startle reflex in rats. In humans, the role of the orbitofrontal cortex is supported by an electrophysiological study using acoustic stimulation in patients with orbitofrontal lesions [Angrilli et al., 2008]. It shows a deficient PPI response in these patients. The ROI approach also indicates that the orbitofrontal cortex is not an exclusive modulator of the startle reflex. It involves the anterior cingulate cortex, the cerebellum, and the thalamus/striatum as well. This replicates the results of prior neuroimaging studies [Campbell et al., 2007; Goldman et al., 2006; Hazlett et al., 1998, 2001, 2008; Kumari et al., 2003a,b,c].

Our data clearly involve the cerebellum in the startle reflex and its modification. This is in line with prior PET and fMRI studies, especially by Timmann and her group [Dimitrova et al., 2002; Pissiota et al., 2002; Timmann et al., 1998]. As part of the core network as identified by the conjunction analysis PA, PPI, and PPF, the left crus1 and lobule VI left are active in our data. These subregions are considered to be involved in the cognitive domain by a recent comprehensive review focusing on cerebellar activation in neuroimaging studies [Stoodley and Schmahmann, 2009]. For the modulated startle responses, other regions of the cerebellum are activated. These are the right lobule VIII and the left lobule X. Especially, the lobule VIII is considered to take part in sensorimotor processing [Stoodley and Schmahmann, 2009]. The F-contrast for differentially activated neural structures during PA, PPI, and PPF identifies activation in the vermis of the cerebellum (Fig. 4a,b). The vermis is implicated in affective processing and behavior [Maschke et al., 2003; Stoodley and Schmahmann, 2009; Timmann et al., 1998]. The cerebellum contributes to the startle reflex and its modification in three domains, in the sensorimotor domain, in the cognitive domain, and in the affective domain.

fMRI data and EMG/EEG data are sampled at a different time frame. How to approach this different temporal solution in data analysis and interpretation is an evolving field of research [Esposito et al., 2009, in press]. For our data, we chose an event-related design and a single trial approach resulting in a startle-data informed fMRI analysis.

In summary, we present a simultaneous MR-compatible startle reflex setup (stimulation and recording online) with a single trial approach in healthy volunteers. This enables a single trial informed fMRI analysis. Deficits in PPI and PPF characterize a range of neuropsychiatric disorders such as schizophrenia, Tourette's syndrome, and Chorea Huntington. As an outlook for further studies, the combined measurement allows for the quantification of these deficits. This prepares the ground for the evaluation of pharmacological approaches to improve the ability to gate out irrelevant stimuli, i.e. by neuroleptic medication in schizophrenia. The startle reflex can be studied across species and is a salient tool for the translation of pharmacologic animal research results to humans.

ACKNOWLEDGMENTS

We thank Jacob Schmitz and his team for their excellent technical support. We would like to thank Barbara Elghahwagi, Petra Engels, and Cordula Kemper for their invaluable assistance during scanning.

REFERENCES

Allen PJ, Polizzi G, Krakow K, Fish DR, Lemieux L (1998): Identification of EEG events in the MR scanner: The problem of pulse artifact and a method for its subtraction. Neuroimage 8:229–239.

Allen PJ, Josephs O, Turner R (2000): A method for removing imaging artifact from continuous EEG recorded during functional MRI. Neuroimage 12:230–239.

Amunts K, Malikovic A, Mohlberg H, Schormann T, Zilles K (2000): Brodmann's areas 17 and 18 brought into stereotaxic space—Where and how variable? Neuroimage 11:66–84.

Amunts K, Kedo O, Kindler M, Pieperhoff P, Mohlberg H, Shah NJ, Habel U, Schneider F, Zilles K (2005): Cytoarchitectonic mapping of the human amygdala, hippocampal region and entorhinal cortex: Intersubject variability and probability maps. Anat Embryol 210:343–352.

Angrilli A, Bianchin M, Radaelli S, Bertagnoni G, Pertile M (2008): Reduced startle reflex and aversive noise perception in

patients with orbitofrontal cortex lesions. Neuropsychologia 46:1179–1184.

Behrens TE, Johansen-Berg H, Woolrich MW, Smith SM, Wheeler-Kingshott CA, Boulby PA, Barker GJ, Sillery EL, Sheehan K, Ciccarelli O, Thompson AJ, Brady JM, Matthews PM (2003): Non-invasive mapping of connections between human thalamus and cortex using diffusion imaging. Nat Neurosci 6:750–757.

Blumenthal TD (1996): Inhibition of the human startle response is affected by both prepulse intensity and eliciting stimulus intensity. Biol Psychol 44:85–104.

Braff DL, Grillon C, Geyer MA (1992): Gating and habituation of the startle reflex in schizophrenic patients. Arch Gen Psychiatry 49:206–215.

Braff DL, Swerdlow NR, Geyer MA (1999): Symptom correlates of prepulse inhibition deficits in male schizophrenic patients. Am J Psychiatry 156:596–602.

Braff DL, Geyer MA, Swerdlow NR (2001): Human studies of prepulse inhibition of startle: Normal subjects, patient groups, and pharmacological studies. Psychopharmacology 156:234–258.

Campbell LE, Hughes M, Budd TW, Cooper G, Fulham WR, Karayanidis F, Hanlon MC, Stojanov W, Johnston P, Case V, Schall U (2007): Primary and secondary neural networks of auditory prepulse inhibition: A functional magnetic resonance imaging study of sensorimotor gating of the human acoustic startle response. Eur J Neurosci 26:2327–2333.

Davis M, Gendelman DS, Tischler MD, Gendelman PM (1982): A primary acoustic startle circuit: Lesion and stimulation studies. J Neurosci 2:791–805.

Diederich A, Colonius H (2008): Crossmodal interaction in saccadic reaction time: Separating multisensory from warning effects in the time window of integration model. Exp Brain Res 186:1–22.

Diederich K, Koch M (2005): Role of the pedunculopontine tegmental nucleus in sensorimotor gating and reward-related behavior in rats. Psychopharmacology 179:402–408.

Dimitrova A, Weber J, Maschke M, Elles HG, Kolb FP, Forsting M, Diener HC, Timmann D (2002): Eyeblink-related areas in human cerebellum as shown by fMRI. Hum Brain Mapp 17:100–115.

Durston S, Davidson MC, Thomas KM, Worden MS, Tottenham N, Martinez A, Watts R, Ulug AM, Casey BJ (2003): Parametric manipulation of conflict and response competition using rapid mixed-trial event-related fMRI. Neuroimage 20:2135–2141.

Eickhoff SB, Stephan KE, Mohlberg H, Grefkes C, Fink GR, Amunts K, Zilles K (2005): A new SPM toolbox for combining probabilistic cytoarchitectonic maps and functional imaging data. Neuroimage 25:1325–1335.

Eickhoff SB, Amunts K, Mohlberg H, Zilles K (2006): The human parietal operculum. II. Stereotaxic maps and correlation with functional imaging results. Cereb Cortex 16:268–279.

Esposito F, Mulert C, Goebel R (2009): Combined distributed source and single-trial EEG-fMRI modeling: Application to effortful decision making processes. Neuroimage 47:112–121.

Esposito F, Aragri A, Piccoli T, Tedeschi G, Goebel R, Di SF (2009): Distributed analysis of simultaneous EEG-fMRI time-series: Modeling and interpretation issues. Magn Reson Imaging 8:1120–1130.

Fendt M (2001): Injections of the NMDA receptor antagonist aminophosphonopentanoic acid into the lateral nucleus of the amygdala block the expression of fear-potentiated startle and freezing. J Neurosci 21:4111–4115.

Filion DL, Dawson ME, Schell AM (1993): Modification of the acoustic startle-reflex eyeblink: A tool for investigating early and late attentional processes. Biol Psychol 35:185–200.

Friston KJ, Fletcher P, Josephs O, Holmes A, Rugg MD, Turner R (1998): Event-related fMRI: Characterizing differential responses. Neuroimage 7:30–40.

Geyer S, Schleicher A, Zilles K (1999): Areas 3a, 3b, and 1 of human primary somatosensory cortex. Neuroimage 10:63–83.

Goldman MB, Heidinger L, Kulkarni K, Zhu DC, Chien A, McLaren DG, Shah J, Coffey CE Jr, Sharif S, Chen E, Uftring SJ, Small SL, Solodkin A, Pilla RS (2006): Changes in the amplitude and timing of the hemodynamic response associated with prepulse inhibition of acoustic startle. Neuroimage 32:1375–1384.

Graham FK (1975): Presidential Address, 1974. The more or less startling effects of weak prestimulation. Psychophysiology 12:238–248.

Hazlett EA, Buchsbaum MS, Haznedar MM, Singer MB, Germans MK, Schnur DB, Jimenez EA, Buchsbaum BR, Troyer BT (1998): Prefrontal cortex glucose metabolism and startle eyeblink modification abnormalities in unmedicated schizophrenia patients. Psychophysiology 35:186–198.

Hazlett EA, Buchsbaum MS, Tang CY, Fleischman MB, Wei TC, Byne W, Haznedar MM (2001): Thalamic activation during an attention-to-prepulse startle modification paradigm: A functional MRI study. Biol Psychiatry 50:281–291.

Hazlett EA, Buchsbaum MS, Zhang J, Newmark RE, Glanton CF, Zelmanova Y, Haznedar MM, Chu KW, Nenadic I, Kemether EM, Tang CY, New AS, Siever LJ (2008): Frontal-striatal-thalamic mediodorsal nucleus dysfunction in schizophrenia-spectrum patients during sensorimotor gating. Neuroimage 42:1164–1177.

Henson RN, Price CJ, Rugg MD, Turner R, Friston KJ (2002): Detecting latency differences in event-related BOLD responses: Application to words versus nonwords and initial versus repeated face presentations. Neuroimage 15:83–97.

Hsieh MH, Swerdlow NR, Braff DL (2006): Effects of background and prepulse characteristics on prepulse inhibition and facilitation: Implications for neuropsychiatric research. Biol Psychiatry 59:555–559.

Koch M, Schnitzler HU (1997): The acoustic startle response in rats—Circuits mediating evocation, inhibition and potentiation. Behav Brain Res 89:35–49.

Kumari V, Gray JA, Ffytche DH, Mitterschiffthaler MT, Das M, Zachariah E, Vythelingum GN, Williams SC, Simmons A, Sharma T (2003a): Cognitive effects of nicotine in humans: An fMRI study. Neuroimage 19:1002–1013.

Kumari V, Gray J, Gupta P, Luscher S, Sharma T (2003b): Sex differences in prepulse inhibition of the acoustic startle response. Pers Individ Dif 34:733–742.

Kumari V, Gray JA, Geyer MA, Ffytche D, Soni W, Mitterschiffthaler MT, Vythelingum GN, Simmons A, Williams SC, Sharma T (2003c): Neural correlates of tactile prepulse inhibition: A functional MRI study in normal and schizophrenic subjects. Psychiatry Res 122:99–113.

Kumari V, Antonova E, Zachariah E, Galea A, Aasen I, Ettinger U, Mitterschiffthaler MT, Sharma T (2005): Structural brain correlates of prepulse inhibition of the acoustic startle response in healthy humans. Neuroimage 26:1052–1058.

Kumari V, Antonova E, Geyer MA, Ffytche D, Williams SC, Sharma T (2007): A fMRI investigation of startle gating deficits in schizophrenia patients treated with typical or atypical antipsychotics. Int J Neuropsychopharmacol 10:463–477.

Lugo E, Doti R, Faubert J (2008): Ubiquitous crossmodal stochastic resonance in humans: Auditory noise facilitates tactile, visual and proprioceptive sensations. PLoS ONE 3:e2860.

Maguire EA, Henson RN, Mummery CJ, Frith CD (2001): Activity in prefrontal cortex, not hippocampus, varies parametrically with the increasing remoteness of memories. Neuroreport 12:441–444.

Maschke M, Erichsen M, Drepper J, Jentzen W, Muller SP, Kolb FP, Diener HC, Timmann D (2003): Cerebellar representation of the eyeblink response as revealed by PET. Neuroreport 14:1371–1374.

McDowell JE, Brown GG, Lazar N, Camchong J, Sharp R, Krebs-Thomson K, Eyler LT, Braff DL, Geyer MA (2006): The neural correlates of habituation of response to startling tactile stimuli presented in a functional magnetic resonance imaging environment. Psychiatry Res 148:1–10.

Morosan P, Rademacher J, Schleicher A, Amunts K, Schormann T, Zilles K (2001): Human primary auditory cortex: Cytoarchitectonic subdivisions and mapping into a spatial reference system. Neuroimage 13:684–701.

Mulert C, Seifert C, Leicht G, Kirsch V, Ertl M, Karch S, Moosmann M, Lutz J, Moller HJ, Hegerl U, Pogarell O, Jager L (2008): Single-trial coupling of EEG and fMRI reveals the involvement of early anterior cingulate cortex activation in effortful decision making. Neuroimage 42:158–168.

Pissiota A, Frans O, Fredrikson M, Langstrom B, Flaten MA (2002): The human startle reflex and pons activation: A regional cerebral blood flow study. Eur J Neurosci 15:395–398.

Plappert CF, Pilz PK, Schnitzler HU (2004): Factors governing prepulse inhibition and prepulse facilitation of the acoustic startle response in mice. Behav Brain Res 152:403–412.

Senkowski D, Schneider TR, Foxe JJ, Engel AK (2008): Crossmodal binding through neural coherence: Implications for multisensory processing. Trends Neurosci 31:401–409.

Stöcker T, Schneider F, Klein M, Habel U, Kellermann T, Zilles K, Shah NJ (2005): Automated quality assurance routines for fMRI data applied to a multicenter study. Hum Brain Mapp 25:237–246.

Stoodley CJ, Schmahmann JD (2009): Functional topography in the human cerebellum: A meta-analysis of neuroimaging studies. Neuroimage 44:489–501.

Swerdlow NR, Geyer MA (1998): Using an animal model of deficient sensorimotor gating to study the pathophysiology and new treatments of schizophrenia. Schizophr Bull 24:285–301.

Swerdlow NR, Braff DL, Geyer MA (1999): Cross-species studies of sensorimotor gating of the startle reflex. Ann N Y Acad Sci 877:202–216.

Swerdlow NR, Geyer MA, Braff DL (2001a): Neural circuit regulation of prepulse inhibition of startle in the rat: Current knowledge and future challenges. Psychopharmacology 156: 194–215.

Swerdlow NR, Karban B, Ploum Y, Sharp R, Geyer MA, Eastvold A (2001b): Tactile prepuff inhibition of startle in children with Tourette's syndrome: In search of an "fMRI-friendly" startle paradigm. Biol Psychiatry 50:578–585.

Takahashi K, Nagai T, Kamei H, Maeda K, Matsuya T, Arai S, Mizoguchi H, Yoneda Y, Nabeshima T, Takuma K, Yamada K (2007): Neural circuits containing pallidotegmental GABAergic neurons are involved in the prepulse inhibition of the startle reflex in mice. Biol Psychiatry 62:148–157.

Timmann D, Musso C, Kolb FP, Rijntjes M, Juptner M, Muller SP, Diener HC, Weiller C (1998): Involvement of the human cerebellum during habituation of the acoustic startle response: A PET study. J Neurol Neurosurg Psychiatry 65:771–773.

Vaidyanathan U, Patrick CJ, Bernat EM (2009): Startle reflex potentiation during aversive picture viewing as an indicator of trait fear. Psychophysiology 46:75–85.

Zavitsanou K, Cranney J, Richardson R (1999): Dopamine antagonists in the orbital prefrontal cortex reduce prepulse inhibition of the acoustic startle reflex in the rat. Pharmacol Biochem Behav 63:55–61.